# Computations of the Contraction Coefficient of Unsymmetrical Bends

R. R. Mankbadi* and S. S. Zaki†
*Cairo University, Cairo, Egypt*

**The Kirchhoff free streamline concept is applied to study two-dimensional potential flow with separation in bends of various area ratios and turning angles. The solution is obtained via successive mapping of the hodograph plane. The flow pattern is studied for the unsymmetric bend and compared to that of the symmetric bend. The calculated values of the coefficient of contraction were found to agree favorably with the measured ones.**

## Nomenclature

$a$ = upstream width of the bend
$b$ = width of downstream contracted flow
$C_c$ = contraction coefficient, $=b/d$
$d$ = downstream width of the bend
$i$ = $\sqrt{-1}$
$L_1$ = length from the inner corner to the upstream uniform flow
$L_2$ = length from the inner corner to the downstream uniform flow
$M$ = bend index, $=\pi/\alpha$
$\bar{q}$ = complex conjugate of the velocity function
$u$ = horizontal velocity component
$U$ = magnitude of velocity along the separated free streamline
$v$ = vertical component velocity
$V$ = upstream uniform velocity
$W$ = complex potential
$\alpha$ = turning angle
$\beta$ = bend ratio, $=a/d$
$\phi$ = potential function
$\psi$ = stream function

## Introduction

FLOW separation in internal and external flows has received much attention because of its significance to estimating the losses in several technologically important problems. The solution of the full Navier-Stokes equation is required in order to predict the onset of separation and the resulting energy dissipation. Such solutions are quite tedious, particularly if the boundaries are not simple ones. The simplicity of potential flow analysis, and its applicability to complicated boundaries, have long led investigators to model real flows by potential ones. Although the potential flow theory cannot predict the energy dissipation resulting from separation, a good estimate of such dissipation can be obtained via a potential flow estimate of the size of the separation bubble and the velocity gradient across it. In addition, determining the pattern of the separated flow enables one to calculate the forcing that acts on the fluids.

Although the inviscid problem is an idealistic one, the infinite Reynolds number limit solution of a viscous flow is usually inviscid. Stewartson[1] and Smith[2,3] have shown that many forms of separation follow Kirchhoff's[4] model. In Kirchhoff's theory, separation is represented through the introduction of a surface of discontinuity that separates the flow into two regions: 1) the main flow where the velocity is continuous and possesses a potential, and 2) a secondary region extending theoretically to infinity and bounded by the surface of discontinuity. The velocity on such surface is assumed to remain constant and is equal to that of the downstream flow at infinity. Kirchhoff[4] has shown that, for the case of a lamina placed perpendicular to a uniform flow, his free streamline theory predicts a drag coefficient in accordance with the measured values. Roshko[5,6] has also proposed an alternative solution for the problem of a wake behind a lamina in which the velocity distribution over the separated free streamline is different from that of Kirchhoff. In Roshko's free streamline model, the velocity at the separation point is greater than that of the undisturbed flow and remains constant along the separated free streamline, which curves gradually until its direction is restored to that of the undisturbed flow. The direction then remains constant, but the velocity decreases to that of the downstream value.

These free streamline theories have proved to be successful in several other applications such as in the case of the flow through a slot in a flat plate[7] and the case of the flow in a right-angle bend[8] to mention only a few. Kirchhoff's asymptotic form is particularly well established in internal flows. Therefore, in the case of separated flow in bends, Kirchhoff's solution is valid for a high Reynolds number.

The present work is concerned with the separated flow in a two-dimensional bend of unequal sides. The turning angle can vary from 0 to $\pi$. The problem is significant to the flow in pipes and channels as well as turbomachine blades. Rather than using the full Navier-Stokes equations, analysis of potential flow with separation is used here. The solution is obtained via successive transformations of the velocity plane—the hodograph—rather than the actual physical plane of the flow. The coefficient of contraction is obtained in terms of the geometrical parameters of the bend. The flow pattern of the unsymmetrical bend is obtained for several turning angles and compared with that of the symmetric bend.

## Formulation

The problem under consideration is that of a steady separated inviscid incompressible flow inside a two-dimensional bend of sharp corners as shown in Fig. 1. The angle $\alpha$ between the two sides of the bend can vary from 0 to $\pi$. For the upstream section of the bend, the width is $a$ and the inlet flow is uniform with a velocity $V$. The downstream side of the bend is of width $d$. The bend is thus geometrically defined by two parameters: the width ratio $\beta=a/d$ and the

Received July 12, 1985; revision received Dec. 16, 1985. 

*Associate Professor, Department of Mechanical Engineering. Member AIAA.
†Graduate Student, Department of Mechanical Engineering.

bend index $M=\pi/\alpha$. Flow separation is assumed to occur at the convex corner A, while no separation is to occur at the concave corner C. At high Reynolds numbers, Smith[3] and Smith and Duck[9] have shown that the cornered channel problem poses a significant upstream interaction that can cause the flow to separate very far upstream on the outer wall B′C of Fig. 1. However, observations indicate that the separation at the inner corner is more severe than that at the outer corner, particularly at lower Reynolds numbers. Therefore, the problem is simplified here by considering only one separation line, starting at the inner corner A. It is required to obtain an analytical function describing the flowfield inside the bend and to calculate the associated flow parameters.

The physical plane of the bend is termed the $z$ plane, where $z=x+iy$ $(i=\sqrt{-1})$. The coordinate axes are placed such that the $x$ axis lies along the upper boundary AD and the $y$ axis originates at the corner point A. Point E is where the full amount of contraction resulting from separation is achieved. Thus, the distance ED′ determines the width $b$ of the downstream contracted flow. BB′ is the section determined by the length $L_1$ measured from A where the upstream flow is uniform. Similarly, DD′ is the section determined by the length $L_2$, where the downstream flow becomes uniform. The fluid is thus bounded by the solid boundaries AB, B′C, and CD′, and by the free streamline AE.

Following Kirchhoff,[4] the free streamline is assumed to be asymptotic extending to infinity, as indicated by the surface AE in Fig. 1. The pressure on the free streamline is constant and has the minimum value in the flow. Hence, the velocity along the separated free streamline is constant and maximum in the flow, which implies that the cavity is convex and excludes closure with a stagnation point or a cusp. The velocity at the point of separation is finite and is equal to that of the flow at the solid boundary at the point of separation. The direction of the separated free streamline far downstream is the same as that of the uniform flow.

Let $w(z)$ be the complex potential where $w$ is defined as

$$w=\phi+i\psi$$

where $\phi$ and $\psi$ are the potential and stream functions, respectively. The complex conjugate of the velocity function $q(z)$ is then given by

$$\bar{q}=qe^{-i\theta}=u-iv=\mathrm{d}w/\mathrm{d}z$$

where $q$ and $\theta$ are the magnitude and direction of the velocity at a given point and $u$ and $v$ are the horizontal and vertical components, respectively.

The solution is obtained here through mapping the velocity plane, the hodograph, rather than the actual physical geometry. The hodograph plane $\xi$ is defined here as

$$\xi=U/\bar{q}=U\mathrm{d}z/\mathrm{d}w \tag{1}$$

where $U$ is the magnitude of the velocity along the separated free streamline, which is taken to be constant. In a polar plot in the $\xi$ plane, the multiply connected flow region BAED′CB′ in the physical plane is mapped into a simply connected one C′EAC, where points C and C′ are at infinity (Fig. 2). The freestream EA is mapped on the $\xi$ plane into a circular arc of unit radius whose center is at the origin. The magnitude of $\bar{q}$ along this arc is constant and equal to $U$, while its direction varies from $-\alpha$ at the point of separation A to zero at E. Points along section ED′ in Fig. 1 map onto a single point in Fig. 2 where $\xi=1$, while points along the upstream section BB′ are mapped onto a single point $\xi=a/b\ \exp(-i\alpha)$. Since C is a stagnation point, it is plotted at infinity.

To transform the circular arc EA into a rectangular boundary, the logarithmic transformation of the form

$$\xi'=\ln(\xi) \tag{2}$$

is used. This transformation maps the interior of CAEC′ in the $\xi$ plane into a semi-infinite strip at the $\xi'$ plane (Fig. 3). The width of this rectangular segment is $-i\alpha$. Points C, B, A, E, and C′ are thus mapped to $(\infty,\ -i\alpha)$, $(\ln a/b,\ -i\alpha)$, $(0,\ -i\alpha)$, $(0,\ 0)$, and $(\infty,\ 0)$, respectively.

The semi-finite rectangular strip in the $\xi'$ plane can be transformed into the upper half of a $\xi''$ plane by using a Schwartz-Christofel transformation of the form

$$\xi''=-\cosh(\pi\xi'/\alpha) \tag{3}$$

which transforms points A and E of the $\xi'$ plane into (1, 0) and $(-1,\ 0)$ in the $\xi''$ plane. Points C′, B, and C are transformed to $(-\infty,\ 0)$, $(L,\ 0)$, and $(\infty,\ 0)$, respectively. $L$ is given by

$$L=\cosh[M\ln(\beta/C_c)] \tag{4}$$

where $C_c$ is the coefficient of contraction defined as

$$C_c=b/d$$

The relation between $L$ and $C_c$ can be recast in the form

$$C_c=\beta\ \exp[-(1/M)\cosh^{-1}L] \tag{5}$$

Since $M$ and $\beta$ are parameters defined through the given bend geometry, the length $L$ is known once $C_c$ is known. $C_c$ will be determined later on through examining the shape of the free streamline.

Along the separated free streamline $\mathrm{d}\psi=0$. Hence, $\mathrm{d}w=\mathrm{d}\phi=(\mathrm{d}\phi/\mathrm{d}s)\mathrm{d}s=U\mathrm{d}s$ where $\mathrm{d}s$ is the distance measured along the streamline. Since in the physical $z$ plane we have

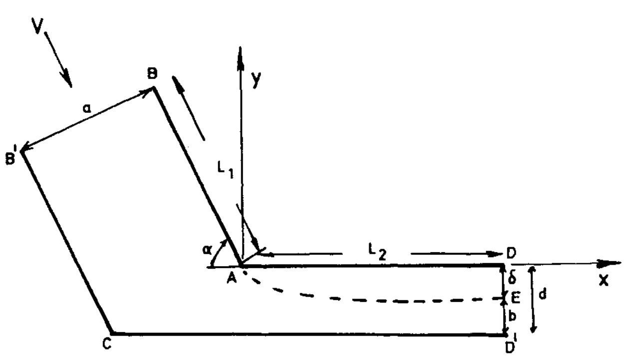


**Fig. 1 Physical plane of the bend.**

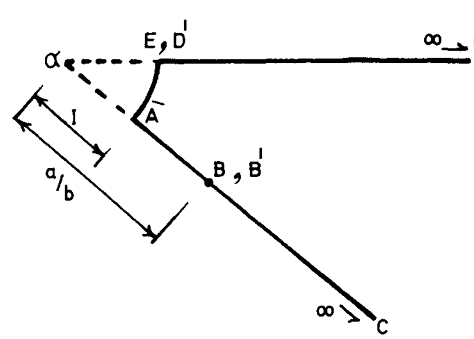


**Fig. 2 Representation of the complex function $U/(\mathrm{d}w/\mathrm{d}z)$ of the flow region BAED′CB′ on the hodograph $\xi$ plane.**

$$dy = ds \sin\theta$$

then

$$dy = \sin\theta \, dw/U \tag{6}$$

to integrate Eq. (6), the potential function $w$ must be specified. $w$ is obtained as follows. It is obvious that all the streamlines in the $\xi''$ plane (Fig. 4) must go from point B′ to point E. The amount of flow entering point E on the real axis of the upper half of $\xi''$ plane equals $aV$. The flowfield in $\xi''$ plane can then be modeled by a point sink at E of strength $aV$ and a point source of the same strength at B′. Hence, the complex potential is given by

$$w(\xi'') = (aV/\pi)\ln[(\xi'' - L)/(\xi'' + 1)] \tag{7}$$

The dimensionless complex potential $w^+$ is defined as

$$w^+(\xi'') = \phi^+ + i\psi^+ = (1/\pi)\ln[(\xi'' - L)/(\xi'' + 1)]$$

where $\phi^+$ and $\psi^+$ are the dimensionless potential and stream functions, respectively, normalized by $aV$.

The complex potential $w(z)$ can then be obtained as follows. Equation (7) is first recast into the form

$$\xi'' = -[\exp(\pi w^+) + L]/[\exp(\pi w^+) - 1] \tag{8}$$

which is combined with Eq. (3), written in the form

$$\xi'' = \cosh\{M[\ln(U dz/dw) + i\alpha]\} \tag{9}$$

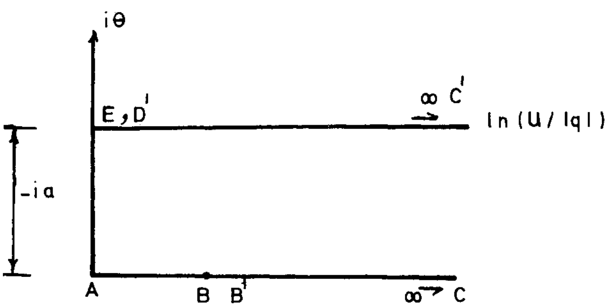


Fig. 3 $\xi'$ plane.

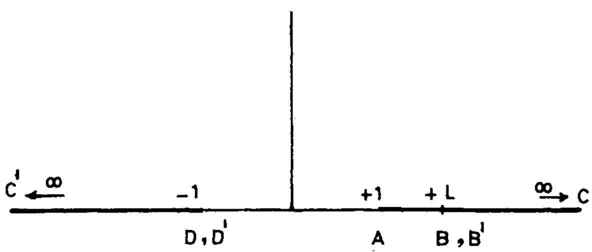


Fig. 4 $\xi''$ plane.

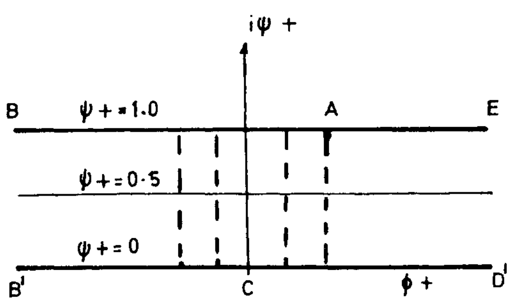


Fig. 5 Complex potential $w^+$ plane.

to yield

$$dw/dz = U\exp\{(-1/M)\cosh^{-1}[F(w^+)] + i\alpha\} \tag{10}$$

where

$$F(w^+) = -[\exp(\pi w^+) + L]/[\exp(\pi w^+) - 1]$$

Rearranging and integrating Eq. (10), one obtains

$$z^+ = \left(\frac{V}{U}\right)\int_{w_0^+}^{w^+} \exp\left\{\frac{1}{M}\cosh^{-1}[F(w^+)] - i\alpha\right\} dw^+ \tag{11}$$

where $z^+ = z/a$. This establishes the relationship between the complex potential function and the physical coordinates.

With the complex potential now determined, the shape of the separated free streamline can be obtained. Substituting Eq. (7) into Eq. (6), one obtains for the free streamline

$$dy = \frac{(aV/\pi U)(L+1)(\sin\theta)}{[(\xi''+1)(\xi''-L)]} d\xi'' \tag{12}$$

Along the free streamline $\xi' = (i\theta)$ and Eq. (3) gives

$$\xi'' = -\cos M\theta \tag{13}$$

Hence

$$\int_0^\delta dy = \frac{a(L+1)VM}{\pi U}\int_\alpha^0 \frac{\sin\theta \sin M\theta}{(L + \cos M\theta)(1 - \cos M\theta)} d\theta$$

which can be written in the form

$$\frac{1}{C_c} = 1 + \frac{M(L+1)}{\pi}\int_0^\alpha \frac{\sin\theta \sin M\theta}{(L + \cos M\theta)(1 - \cos M\theta)} d\theta \tag{14}$$

The $\xi''$ transformation is thus complete, which when combined with the complex potential $w(z)$, provides the solution of the flowfield in the $z$ plane.

## Results and Discussions

By taking $\psi^+$ to be zero along B′CD′ in the physical $z$ plane, then $\psi^+ = 1$ on BAE. A mesh is constructed in the $w^+$ plane bounded by the streamline B′CD′ where $\psi^+ = 0$ and the streamline BAE where $\psi^+ = 1$ (see Fig. 5). A step of $\Delta\psi^+ = 0.1$ is taken to construct several streamlines. The potential function $\phi^+$ is taken to be zero at the stagnation point C. Other equipotential lines are constructed such that they are orthogonal to $\psi^+$ with a step of $\Delta\phi^+ = 0.1$. The

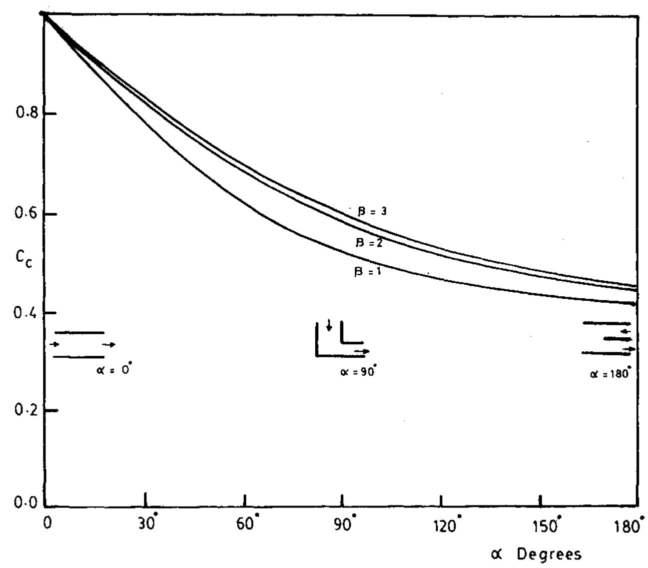


Fig. 6 Contraction coefficient $C_c$ against the bend angle $\alpha$ for various bend ratios, $\beta = a/d$.

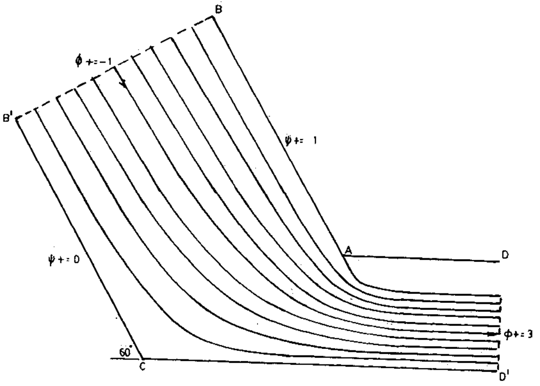


a) $\alpha = 60$ deg.

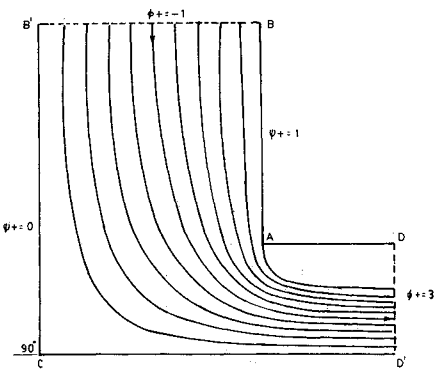


b) $\alpha = 90$ deg.

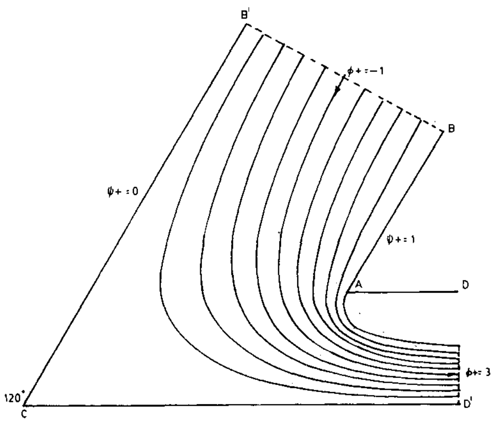


c) $\alpha = 120$ deg.

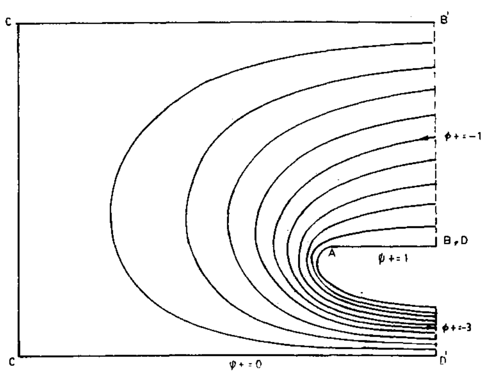


d) $\alpha = 180$ deg.

**Fig. 7 Streamlines for unsymmetric bend of a bend ratio, $\beta = 2$.**

a) $\alpha = 60$ deg.

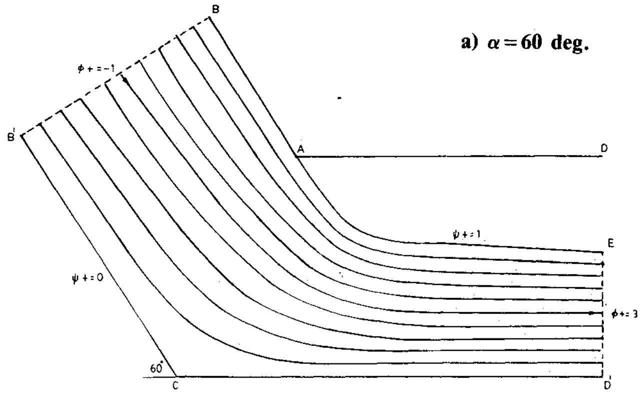


b) $\alpha = 90$ deg.

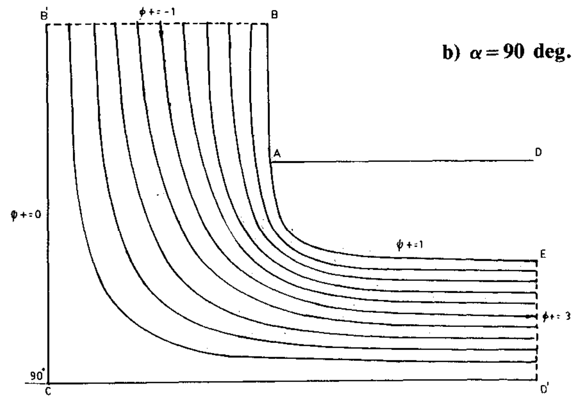


c) $\alpha = 120$ deg.

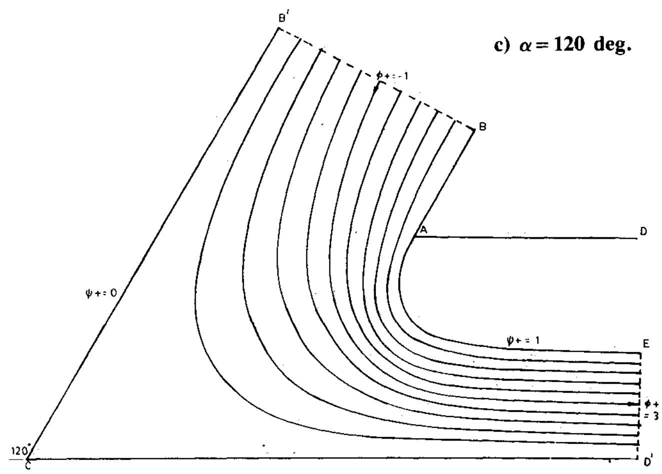


**Fig. 8 Streamlines for symmetric bend, $\beta = 1$.**

lengths $L_1$ and $L_2$ are assumed to be infinity. But $\phi^+ = -1$ was found to produce an almost uniform upstream flow. Thus, section BB′ and the length $L_1$ are taken where $\phi^+ = -1$. Similarly, the downstream section ED′ where the flow is uniform is achieved at $\phi^+ = 3$. With this mesh constructed, the integral of Eq. (11) is performed and the location of a given streamline or equipotential line in the $z$ plane is determined. In the actual computation of Eq. (11), the inverse hyperbolic function is written in terms of the natural logarithm, which is a multiple valued function. The branch cut for the logarithmic function was determined such that the transformation remains comformable and single valued. Therefore, for negative values of $\phi^+$, the principle value of the logarithm was taken, while for positive values of $\phi^+$, $-2\pi i$ was added to the principal value.

The coefficient of contraction $C_c$ calculated according to Eq. (14) is shown in Fig. 6 vs turning angle $\alpha$ for several bend ratios. Since $\alpha = 0$ and $\pi$ are singular points, they were

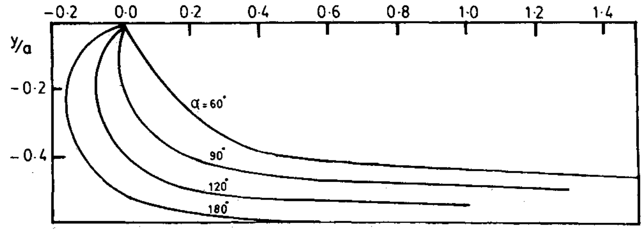


a) Symmetric bend, $\beta = 1$.

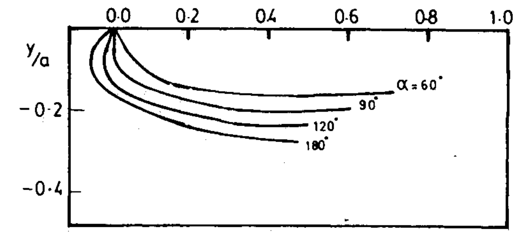


b) Unsymmetric bend, $\beta = 2$.

**Fig. 9 Shape of the free streamline at different bend angles.**

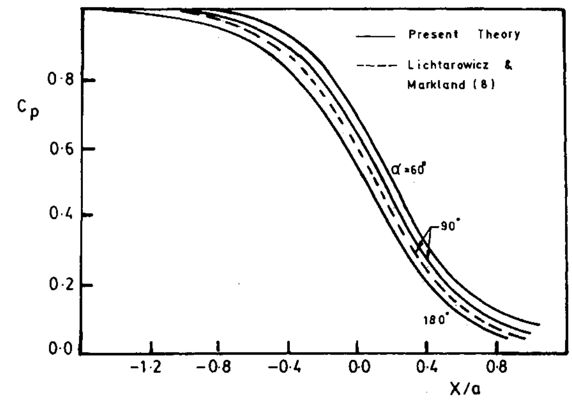


**Fig. 10 Pressure coefficient $C_p$ along CD′ at different bend angles in comparison with Lichtarowicz and Merkland's[8] results, $C_p = (P - P_E)/(\frac{1}{2}\rho U^2)$.**

replaced in the actual computations by 0.1 and 0.99 $\pi$, respectively. The figure shows that $C_c$ is a decreasing function of $\alpha$. The effect of $\alpha$ on $C_c$ is more pronounced for small angles than for large. For the case of a right-angled symmetric bend, ($\beta = 1$, $\alpha = 90$ deg), the present calculation gives $C_c = 0.5231$. Using Roshko's free streamline model,[5,6] Lichtarowicz and Markland[8] obtained $C_c = 0.526$. The corresponding experimental value of Heskestad[10] is 0.526. For an unsymmetric right-angled bend of $\beta = 2$, the present calculation gives $C_c = 0.591$, which corresponds to the theoretical value $C_c = 0.59$ of Lichtarowicz and Markland[8] and to the experimental value $C_c = 0.6$ of Heskestad.[10] The figure also shows that changing $\beta$ from 1 to 2 has a pronounced effect on increasing the coefficient of contraction, but further increase in $\beta$ has little effect on the contraction coefficient.

The streamlines of unsymmetric bend of $\beta = 2$ are shown in Fig. 7 for several bend angles. The figure shows that the stagnation region bounded by $\psi^+ = 0$ and 0.1 around the corner C increases with $\alpha$. The figure also shows that the curvature of the streamlines increases with $\alpha$. This indicates that the effect of separation is more severe and localized for large bend angles. The velocity distribution can be inferred from the spacing between the streamlines. $\psi^+ = 0.5$ is the streamline that divides the flow into two equal parts. Figure 7 shows that for all the turning angles considered, the flow is always accelerating for $\psi^+ > 0.5$, while for $\psi^+ < 0.5$, the flow first decelerates and then accelerates again.

For the purpose of comparison, the streamlines of the flow inside a symmetric bend is shown in Fig. 8 for several bend angles. The figure shows that for all the bend angles considered, the stagnation zone of the unsymmetric bend of $\beta = 2$ is less than that of the symmetric bend of the same bend angle, as would also be implied from Fig. 6 for $C_c$. The upstream section where the flow begins to be influenced $L_1$ is larger for the symmetric bend than for the unsymmetric bend. The downstream section at which the flow becomes uniform $L_2$ is reached sooner for the unsymmetric bend than for the symmetric one.

The separated free streamline is plotted in Fig. 9 for several bend angles for the symmetric and unsymmetric bends. The figure shows that the curvature of the free streamline increases with $\alpha$. In the actual flow of a bend in a pipe, the downstream flow may not remain contracted, but rather might expand to fill the downstream pipe and thus close the separation "bubble." However, in a chocked flow condition, the free streamline will extend to infinity as postulated in the present method. Therefore, its present solution is a good approximation of the real chocked flow at high Reynolds numbers.

The pressure distribution along the lower side CD′ of the symmetrical bend is shown in Fig. 10 for several bend angles. The results of Lichtarowicz and Markland[8] at $M = 2$ are also shown on the same figure. The figure shows that the pressure along this side decreases with increasing bend angle.

## Conclusions

The separated potential flow of unsymmetric bend of sharp corners has been obtained through successive mapping of the velocity plane. The method ignores the upstream interactions and is limited to cases where there are no reattachments. The method has the advantage of being applicable to bends with arbitrary bend ratios and turning angles. The calculated coefficient of contraction was found to be in good agreement with the measured values. The coefficient of contraction decreases with increasing turning angle and increases as the bend's reduction ratio increases to a certain limit, beyond which further increase in the bend's ratio has little effect on the coefficient of contraction. The size of the stagnation zone increases as the turning angle increases and decreases as the bend's reduction ratio increases. The pressure along the outer boundary of the bend decreases as the turning angle increases.

## References

[1]Stewartson, K., "Multistructured Boundary Layers on Flat Plates and Related Bodies," *Advances in Applied Mechanics*, Vol. 14, 1974, p. 145.

[2]Smith, F. T., "Laminar Flow of an Incompressible Fluid Past a Bluff Body: The Separation, Reattachment, Eddy Properties and Drag," *Journal of Fluid Mechanics*, Vol. 92, 1979, p. 171.

[3]Smith, F. T., "On the High Reynolds Number Theory of Laminar Flows," *Journal of Applied Mechanics*, Vol. 28, 1982.

[4]Kirchhoff, G., "Zur Theorie freir Flüssigkeitsstrahlen," *Journal Reine Angew. Math.*, Vol. 70, 1869, pp. 289-298.

[5]Roshko, A., "On the Wake and Drag of Bluff Bodies," *Journal of the Aeronautical Sciences*, Vol. 22, 1955, pp. 124-132.

[6]Roshko, A., "Experiments on the Flow Past a Circular Cylinder at Very High Reynolds Number," *Journal of Fluid Mechanics*, Vol. 10, pp. 345-356.

[7]Milne-Thomson, L. M., *Theoretical Hydrodynamics*, Macmillan, New York, 1949.

[8]Lichtarowicz, A. and Markland, E., "Calculation of Potential Flow with Separation in a Right-Angled Elbow with Unequal Branches," *Journal of Fluid Mechanics*, Vol. 17, 1963, pp. 596-606.

[9]Smith, F. T. and Duck, P. W., "On the Severe Non-Symmetric Constriction, Curving, or Cornering of Channel Flows," *Journal of Fluid Mechanics*, Vol. 98, 1980, pp. 727-753.

[10]Heskestad, G., "Two-Dimensional Milter-Bend Flow," *Transactions of ASME, Journal of Basic Engineering*, Vol. 93, Sept. 1971, pp. 433-443.